Journal of Solid Mechanics Vol. 9, No. 2 (2017) pp. 338-350

Axisymmetric Buckling Analysis of Porous Truncated Conical Shell Subjected to Axial Load

M. Zarghami Dehaghani , M.Jabbari *

Department of Mechanical Engineering, South Tehran Branch, Islamic Azad University, Tehran, Iran

Received 2 March 2017; accepted 25 April 2017

ABSTRACT

This paper studied Buckling analysis of porous truncated conical shell subjected to axial load. It is considered that a fluid undrained between porous material and the Porous material properties vary across the thickness of shell with a specific function also assumed that the edge of the shell is simply supported. The governing equations are based on the Sanders kinematics equations and the first-order shell theory and by using of variational formulations. The general mechanical non-linear equilibrium and linear stability equations are derived. At the end, the result of dimensionless buckling critical load ratio dimensionless thickness in different condition such as variation in thickness, porosity and angle of conical shell is investigated. The mechanical load results are verified by the known results in the literature.

Keywords : Axisymmetric; Porous material; Buckling analysis; Conical shell; Axial load.

1 INTRODUCTION

THE biot model of a fluid-filled porous material is composed on the conceptual model of a coherent solid structure and a freely moving pore fluid (in other words both solid and fluid or gas phases are fully connected). Porous material frequently found in nature, such as wood, stone, and layers of dust. Detournay and Cheng [1] studied fundamentals of poroelasticity. Seide [2,3] studied the buckling of conical shells under the axial loading. Singer [4] considered the buckling of conical shells under the axisymmetrical external pressure. Buckling of the stiffened conical shells under hydrostatic pressure is studied by Baruch and Singer [5]. Baruch et al. [6] studied the buckling of conical shells under the hydrostatic pressure and the buckling loads of axially compressed conical shells for different sets of boundary conditions [7]. Singer [8,9] analyzed the buckling of orthotropic conical shells. Weigarten and Seide [10] studied the stability of conical shells under the axial compression and external pressure. The same authors considered the stability of conical shells under the combined axial compression and internal pressure [11]. Ari-Gur et al. [12] analyzed the buckling of cylindrical shell under combined loading. They considered a cylindrical shell under axial preload, nonuniform heating and torque. Lu and Chang [13] studied the thermal buckling of conical shells. They used the Galerkin method for integrating the equilibrium equations in their analysis. Tani [14] presented a solution on the buckling of conical shell under combined pressure and heating loads. Free vibration and buckling behavior of FG truncated conical shells subjected to thermal loads is investigated by Bhangale et al. [15] based on the first order shear deformation theory. The effects of initial stresses on the frequencies of the FG shells are studied. Thermoelastic stability analysis of FG truncated conical shells is presented by Sofiyev [16]. Modified Donnell type stability and compatibility equations are derived and the Galerkin method is

*Corresponding author. Tel.: +98 912 932 2698.
E-mail address: : *M_Jabbari@azad.ac.ir* (M.Jabbari).

applied to obtain the closed-form solution. The instability of FG truncated conical shells subjected to thermal and mechanical loads is analyzed based on the classical shell theory and the Sanders nonlinear kinematics relations by Naj et al. [17]. In a series of works Sofiyev studied the buckling of FG truncated conical shells under various mechanical loads, including hydrostatic pressure, external pressure, and combined axial tension and hydrostatic pressure (Sofiyev et al. [18] and Sofiyev [19,20]). By applying the Galerkin method to stability and compatibility equations, the critical buckling load of the shell is obtained. Recently, Sofiyev [21, 22] presented the thermal and mechanical buckling analysis of FG circular shells resting on a two-parameters elastic foundation by solving the eigen-value problem. The critical buckling loads with and without elastic foundation are obtained using the Galerkin method. Bich et al. [23] studied the instability of FG conical panels based on the classical thin shell theory under axial compression, external pressure, and combination of them. The effects of the initial imperfections on the buckling behavior of FG truncated conical shells are illustrated by Sofiyev [24]. Superposition and Galerkin methods are applied to the modified nonlinear Donnell type stability and compatibility equations and the upper and lower critical axial loads are obtained. Applying the Galerkin method to the governing equations which are based on higher order shear deformation shell theory, results in a closed form solution for the critical buckling temperature difference. In another study, Mirzavand and Eslami [25] Using the variational approach, equilibrium and stability equations are obtained based on the classical shell theory and the Sanders nonlinear kinematics relations. Jabbari et al. [26] studied the buckling analysis of soft ferromagnetic FG circular plates made of poro material. Jabbari et al. [27] studied the thermal buckling of radially solid circular plate made of porous material with piezoelectric actuator layers presented. Jabbari et al. [28] studied the buckling analysis of radially solid circular plate made of porous material bounded with the layers of piezoelectric actuators. Studied axi-symmetrical deflection and buckling of circular porous-cellular plate by Magnucka-Blandzi [29]. Studied failure by buckling mode of the pore-strut for isotropic three-dimensional reticulated porous metal foams under different compressive loads [30]. Presented mechanical and thermal stability of eccentrically stiffened functionally graded conical shell panels resting on elastic foundations and in thermal environment [31] the shell is a porous material that a fluid undrained between Porous and simply supported at both ends and it is assumed to be subjected to a uniform axial load. The prebuckling forces are obtained by considering membrane solutions of linear equilibrium equations. Applying the Galerkin method to the stability equations results in an eigen-value problem which provides the critical buckling axial load and finally results are presented.

2 DERIVATION OF THE GOVERNING EQUATIONS

Consider a truncated conical shell of thickness h and half apex angle β made of porous material where the curvilinear coordinate system is defined as (x,θ,z), and the displacement components of the middle surface are u, v and w along the meridian, tangential and lateral directions, respectively. The geometry of shell is shown in Fig.1 the relationship between E and z for porous shell is assumed functionally.

$$\begin{aligned} E(z) &= E_0\left[1-e_1\cos\left(\frac{\pi(z+\frac{h}{2})}{h}\right)\right] \\ G(z) &= G_0\left[1-e_1\cos\left(\frac{\pi(z+\frac{h}{2})}{h}\right)\right] \\ e_1 &= 1-\left(\frac{E_1}{E_0}\right)=1-\left(\frac{G_1}{G_0}\right) \end{aligned} \tag{1}$$

where e_1 is the coefficient of shell porosity $0<e_1<1$, E_1 and E_0 Young's modulus of elasticity at $z=-h/2$ and $z=h/2$, respectively, and G_1 and G_0 are the shear modulus at $z=-h/2$ and $z=h/2$, respectively. The relationship between the modulus of elasticity and shear modulus for $j=0$ and 1 is $E_j=2G_j(1+v)$ and ν is Poisson's ratio, which is assumed to be constant across the shell thickness. Mechanical properties of the porous material vary across the thickness of the shell, ($G_0 \geq G_1$).

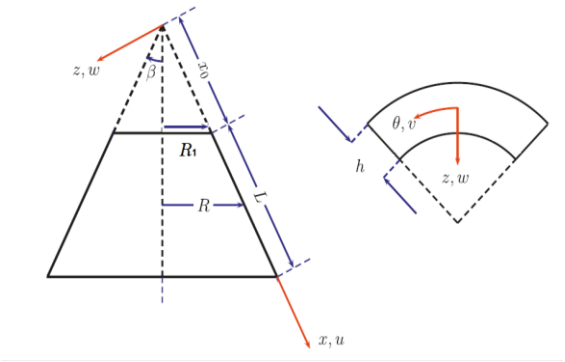

Fig.1
Coordinate and Geometry system of a porous conical shell.

2.1 Basic equations

The linear poroelasticity theory of Biot has two features

1. An increase of pore pressure induces a dilation of pore.
2. Compression of the pore causes a rise of pore pressure.

The stress–strain relation for porous material of the shell are written as following:

$$\bar{\sigma}_{ij} = 2G\bar{\varepsilon}_{ij} + \frac{2G\nu_u}{1-2\nu_u}\bar{\varepsilon}\delta_{ij} - p_p\alpha\delta_{ij} \tag{2}$$

$$\Delta\bar{\varepsilon}_{kk} = \frac{\Delta\bar{\sigma}_{kk}}{3K} + \frac{\alpha\Delta p_p}{K} \tag{3}$$

where

$$p_p = M[\zeta - \alpha\bar{\varepsilon}_{jj}] \tag{4}$$

$$M = \frac{2G(\nu_u - \nu)}{\alpha^2(1-2\nu_u)(1-2\nu)} \tag{5}$$

Here, p_p is pore fluid pressure, M is Biot's modulus, ν_u is undrained Poisson's ratio $\nu < \nu_u < 0.5$, α is the Biot coefficient of effective stress $0 < \alpha < 1$, K is bulk modulus $(K = 2G(1+\nu_u / 3(1-2\nu_u)))$, ζ is variation of fluid volume content, and ε is the volumetric strain. The two dimensional stress-strain law for plane-stress condition in the curvilinear coordinates for the undrained condition ($\zeta = 0$) is given by

$$p_p = M[-\alpha\bar{\varepsilon}_{jj}] \tag{6}$$

And by simplification, Eq. (2) in curvilinear coordinates can be written as:

$$\begin{aligned}\bar{\sigma}_{xx} &= A_1\bar{\varepsilon}_{xx} + B_1\bar{\varepsilon}_{\theta\theta}\\ \sigma_{\theta\theta} &= A_1\bar{\varepsilon}_{\theta\theta} + B_1\bar{\varepsilon}_{xx}\\ \bar{\sigma}_{x\theta} &= G\bar{\gamma}_{x\theta}\end{aligned} \tag{7}$$

where the constants are

$$A_1=\left[\begin{array}{l}\dfrac{\mathrm{E}}{1-\nu_u{}^2}-\left(\dfrac{4G(z)^2\,\nu_u{}^2}{1-4\nu_u+\nu_u{}^2}\dfrac{1-\nu_u{}^2}{E}\right)\\ +\left((1-\nu_u)\dfrac{2G(z)(\nu_u-\nu)}{(1-2\nu_u)(1-2\nu)}\left(1+\dfrac{n_2}{n_1}\right)\right)\end{array}\right]$$

$$B_1=\left[\frac{2G(z)\,\nu_u(1-\nu_u)}{1-2\nu_u}+\frac{2G(z)(\nu_u-\nu)(1-\nu_u)\left(1+\dfrac{n_2}{n_1}\right)}{(1-\nu_u)(1-2\nu)}\right] \tag{8}$$

$$n_1=2G(z)+\frac{2G(z)\,\nu_u}{1-2\nu_u}+\frac{2G(z)\left(\nu_u-\nu\right)}{\left(1-2\nu_u\right)\left(1-2\nu\right)}$$

$$n_2=\frac{2G(z)\left(\nu_u-\nu\right)}{\left(1-2\nu_u\right)\left(1-2\nu\right)}+\frac{2G(z)\,\nu_u}{1-2\nu_u}$$

The shell is assumed to be thin, and according to the Love–Kirchhoff assumptions, planes normal to the median surface are assumed to remain plane after deformation. Thus, shear deformations normal to the shell are disregarded. Using first-order shell theory, strain components at distance z from the middle plane are given in matrix form as:

$$\begin{bmatrix}\overline{\varepsilon_{xx}}\\ \overline{\varepsilon_{\theta\theta}}\\ \overline{\gamma_{x\theta}}\end{bmatrix}=\begin{bmatrix}\varepsilon_{xx}\\ \varepsilon_{\theta\theta}\\ \gamma_{x\theta}\end{bmatrix}+z\begin{bmatrix}k_{xx}\\ k_{\theta\theta}\\ 2k_{x\theta}\end{bmatrix} \tag{9}$$

where $\overline{\varepsilon_{xx}}$, $\overline{\varepsilon_{\theta\theta}}$ and $\overline{\gamma_{x\theta}}$ are the strain components along the x, θ and z-directions, respectively. Here, ε_{xx}, $\varepsilon_{\theta\theta}$ and $\gamma_{x\theta}$ are the middle plane strain components and k_{xx}, $k_{\theta\theta}$ and $k_{x\theta}$ are bending and twisting curvatures with respect to the x- and θ-axes, respectively. The relations between the middle plane strains and curvatures with the displacement components according to the Sanders assumption strain–displacement relations, are obtained as:

$$\begin{aligned}
\varepsilon_{xx}&=u_{,x}+\frac{1}{2}w_x{}^2\\
\varepsilon_{\theta\theta}&=\frac{v_{,\theta}}{x\,\sin\beta}+\frac{u}{x}+\frac{w}{x\,\tan\beta}+\frac{1}{2}\left(-\frac{w_{,\theta}}{x\,\sin\beta}+\frac{v}{x\,\tan\beta}\right)^2\\
\gamma_{x\theta}&=v_{,x}+\frac{u_{,\theta}}{x\,\sin\beta}-\frac{v}{x}+\left(\frac{w_{,\theta}}{x\,\sin\beta}-\frac{v}{x\,\tan\beta}\right)w_x\\
k_{xx}&=\left(w_{,xx}\right)\\
k_{\theta\theta}&=\left(\frac{-w_{,\theta\theta}+\cos\beta v_{,\theta}-x\,\sin^2\beta\left(w_{,x}\right)}{x^2\sin^2\beta}\right)\\
k_{x\theta}&=\left(\frac{w_{,\theta}-x\,w_{,x\theta}-\cos\beta v+\dfrac{x}{2}\cos\beta v_{,x}}{x^2\sin\beta}\right)
\end{aligned} \tag{10}$$

where (u,v,w) represent the corresponding components of the displacement of a point on the middle shell surface and (,) indicates partial differentiation. The force and moment resultants of conical shell according to the first order shell theory are

$$N_{ij} = \int_{-h/2}^{h/2} \overline{\sigma_{ij}}\, dz \qquad M_{ij} = \int_{-h/2}^{h/2} \overline{\sigma_{ij}}\, z\, dz \tag{11}$$

Substituting Eqs. (7) in Eqs. (11) yield

$$\begin{aligned}
N_{xx} &= 2A_2\, \varepsilon_{xx} + A_3\, k_{xx} + B_2\, \varepsilon_{\theta\theta} + B_3\, k_{\theta\theta} \\
N_{\theta\theta} &= 2A_2\, \varepsilon_{\theta\theta} + A_3\, k_{\theta\theta} + B_2\, \varepsilon_{xx} + B_3\, k_{xx} \\
N_{x\theta} &= D_2\, \gamma_{x\theta} + 2D_3\, k_{x\theta} \\
M_{xx} &= A_3\, \varepsilon_{xx} + 2A_4\, k_{xx} + B_3\, \varepsilon_{\theta\theta} + B_4\, k_{\theta\theta} \\
M_{\theta\theta} &= A_3\, \varepsilon_{\theta\theta} + 2A_4\, k_{\theta\theta} + B_3\, \varepsilon_{xx} + B_4\, k_{xx} \\
M_{x\theta} &= D_3\, \gamma_{x\theta} + 2D_4\, k_{x\theta}
\end{aligned} \tag{12}$$

The coefficients are given in the Appendix.

2.2 Strain energy

The total potential energy for porous conical shell can be written as:

$$U = \frac{1}{2}\int \overline{\sigma}_{ij}\, d\,\overline{\varepsilon}_{ij}^{\,E}\, dV \tag{13}$$

where $\varepsilon_{ij}^{\,E}$ is elastic strain. Elastic strain energy for porous materials is comprised of elastic strain energy for solid body and fluid in pores. Substituting Eq. (4) into Eq. (2) in the undrained condition, strain energy is obtained as:

$$\overline{\varepsilon}_{ii} = \frac{(1-\alpha\beta)}{3K}\overline{\sigma}_{ii} \tag{14}$$

Here, $(1-\alpha B)$ is relation between drained bulk modulus and undrained bulk modulus, αB is coupling between pore fluid effects and macroscopic deformation and B is skepton coefficient. By substituting $\overline{\sigma}_{kk} = 3K\overline{\varepsilon}^{E}_{kk}$ in Eq. (14) gives

$$\varepsilon_{ii}^{\,E} = \frac{1}{(1-\alpha\beta)}\varepsilon_{ii} \tag{15}$$

The total potential energy for porous conical shell can be written as:

$$U = \frac{1}{2}\iiint_{\frac{-h}{2}}^{\frac{h}{2}} \left(\frac{\overline{\varepsilon_{xx}}}{1-\alpha\beta}\overline{\sigma_{xx}} + \frac{\overline{\varepsilon_{\theta\theta}}}{1-\alpha\beta}\overline{\sigma_{\theta\theta}} + \overline{\sigma_{x\theta}}\,\overline{\gamma_{x\theta}} \right) x\, \sin\beta\, dx\, d\theta\, dz \tag{16}$$

And by substituting strain-stress relations

$$U = \frac{1}{2}\iiint_{\frac{-h}{2}}^{\frac{h}{2}} \left(\frac{\overline{\varepsilon_{xx}}}{1-\alpha\beta_1}\left(A_1\,\overline{\varepsilon_{xx}} + B_1\,\overline{\varepsilon_{\theta\theta}}\right) + \frac{\overline{\varepsilon_{\theta\theta}}}{1-\alpha\beta}\left(A_1\,\overline{\varepsilon_{\theta\theta}} + B_1\,\overline{\varepsilon_{xx}}\right) + G\,\overline{\gamma_{x\theta}}\,\overline{\gamma_{x\theta}} \right) x\, \sin\beta\, dx\, d\theta\, dz \tag{17}$$

In which

$$U=\iint\left[\begin{array}{l}A_2\left(\varepsilon_{xx}{}^2+\varepsilon_{\theta\theta}{}^2\right)+B_2\left(\varepsilon_{xx}\varepsilon_{\theta\theta}\right)+\frac{1}{2}D_2\,\gamma_{x\theta}{}^2+A_3\left(k_x\varepsilon_{xx}+k_\theta\varepsilon_{\theta\theta}\right)\\+B_3\left(k_\theta\varepsilon_{xx}+k_x\varepsilon_{\theta\theta}\right)+2D_3\,k_{x\theta}\,\gamma_{x\theta}+A_4\left(k_x{}^2+k_\theta{}^2\right)+B_4\left(k_x k_\theta\right)+2D_2 k_{x\theta}{}^2\end{array}\right]x\,\sin\beta\,dx\,d\theta \tag{18}$$

2.3 Stability equations

The equilibrium equations are derived using the functional of potential energy equation of U Eq. (18) and employing the Euler equations. In the functional of total potential energy, the membrane and bending are included. For a conical shell the equilibrium equations, using the variational principle, are derived as:

$$\begin{aligned}&\left(xN_x\right)_{,x}+\frac{1}{\sin\beta}N_{x\theta,\theta}-N_\theta=0\\&\frac{1}{\sin\beta}N_{\theta,\theta}+\left(xN_{x\theta}\right)_{,x}+N_{x\theta}-\cot\beta\left(N_{x\theta}\,\beta_x+N_\theta\,\beta_\theta\right)\\&+\cot\beta\left(M_{x\theta,x}+\frac{2}{x}M_{x\theta}\right)+\frac{M_{\theta,\theta}}{x\,\tan\beta\sin\beta}=0\\&\left(xM_x\right)_{,xx}+\frac{1}{x\,\sin^2\beta}M_{\theta,\theta\theta}-M_{\theta,x}+\frac{2}{x\,\sin\beta}\left(xM_{x\theta,\theta}\right)_{,x}-N_\theta\cot\beta\\&-\left[\left(xN_x\,\beta_x+xN_{x\theta}\,\beta_\theta\right)_{,x}+\frac{1}{\sin\beta}\left(N_{x\theta}\,\beta_x+N_\theta\,\beta_\theta\right)_{,\theta}\right]=0\end{aligned} \tag{19}$$

And

$$\begin{aligned}\beta_x&=-w_{,x}\\\beta_\theta&=-\frac{w_{,\theta}}{x\,\sin\beta}+\frac{v}{x\,\tan\beta}\end{aligned} \tag{20}$$

In Eqs. (20) β_θ and β_x are the rotations of the normal to the middle surface about the x and θ-axes, respectively. The stability equations of the conical shell are derived using the adjacent equilibrium criterion. We assume u_0,v_0 and w_0 as the displacement components of the equilibrium state and u_1,v_1 and w_1 as the virtual displacements corresponding to a neighboring state. The displacement components of the neighboring state are

$$\begin{aligned}u&\to u_0+u_1\\v&\to v_0+v_1\\w&\to w_0+w_1\end{aligned} \tag{21}$$

According to the adjacent equilibrium criterion in the neighboring state of equilibrium, the stability equations are found. Similar to Eqs. (21), the stress and moment resultants are found to be the sum of those related to the equilibrium and neighboring states as:

$$\left(N_i,M_i\right)=\left(N_{i0},M_{i0}\right)+\left(N_{i1},M_{i1}\right),\ i=xx,\theta\theta,x\theta \tag{22}$$

Substituting relations (21) and (22) in Eqs. (19), collecting the second order terms, the stability equations are obtained as:

$$
\begin{aligned}
&\left(xN_{x1}\right)_{,x}+\frac{1}{\sin\beta}N_{x\theta1,\theta}-N_{\theta1}=0\\
&\frac{1}{\sin\beta}N_{\theta1,\theta}+\left(xN_{x\theta_1}\right)_{,x}+N_{x\theta1}-\cot\beta\left(N_{x\theta0}\,\beta_{x1}+N_{\theta0}\,\beta_{\theta1}\right)\\
&+\cot\beta\left(M_{x\theta1,x}+\frac{2}{x}M_{x\theta1}\right)+\frac{M_{\theta1,\theta}}{x\,\tan\beta\sin\beta}=0\\
&\left(xM_{x1}\right)_{,xx}+\frac{1}{x\,\sin^2\beta}M_{\theta1,\theta\theta}-M_{\theta1,x}+\frac{2}{x\,\sin\beta}\left(xM_{x\theta1,\theta}\right)_{,x}-N_{\theta1}\cot\beta\\
&-\left[\left(xN_{x0}\,\beta_{x1}+xN_{x\theta0}\,\beta_{\theta1}\right)_{,x}+\frac{1}{\sin\beta}\left(N_{x\theta0}\,\beta_{x1}+N_{\theta0}\,\beta_{\theta1}\right)_{,\theta}\right]=0
\end{aligned}
\tag{23}
$$

The subscript 0 refers to the equilibrium state and subscript 1 refers to the stability state. The terms with the subscript 0 are the solution of the equilibrium equations for the given load. In which the linear forms of strains and curvatures are given as:

$$
\begin{aligned}
&\varepsilon_{xx1}=\left(u_{1,x}\right)\\
&\varepsilon_{\theta\theta1}=\left(\frac{v_{1,\theta}}{x\,\sin\beta}+\frac{u_1}{x}+\frac{w_1}{x\,\tan\beta}\right)\\
&\gamma_{x\theta1}=\left(v_{1,x}+\frac{u_{1,\theta}}{x\,\sin\beta}-\frac{v_1}{x}\right)\\
&k_{xx1}=\left(w_{1,xx}\right)\\
&k_{\theta\theta1}=\left(\frac{-w_{1,\theta\theta}+\cos\beta v_{1,\theta}-x\,\sin^2\beta\left(w_{1,x}\right)}{x^2\sin^2\beta}\right)\\
&k_{x\theta1}=\left(\frac{w_{1,\theta}-x\,w_{1,x\theta}-\cos\beta v_1+\frac{x}{2}\cos\beta v_{1,x}}{x^2\sin\beta}\right)
\end{aligned}
\tag{24}
$$

For simplicity, the membrane solution of the equilibrium equations are considered [32]. For this aim, all the moment and rotation terms must be set equal to zero in the equilibrium equations. By solving the membrane form of Equilibrium equations, it is found that

$$
N_{x0}=-\frac{P_{cr}}{x\,\pi\sin2\beta},\qquad N_{\theta0}=0\ ,\qquad N_{x\theta0}=0
\tag{25}
$$

Substituting Eqs. (24), (20) into Eqs. (12), and (12), (25) into Eqs. (23), the stability equations in terms of the displacement components are derived.

2.4 Axisymmetric buckling

Up to this point, it was assumed that the buckling mode is not axisymmetric. In this section we will consider the axisymmetric mode in which *v*, the displacements of mid-surface in circumferential direction is equated to zero.

2.5 Boundary conditions

Consider a conical shell with the simply supported boundary edges. The boundary conditions are assumed as [6]

$$
\begin{aligned}
&u_1 = v_1 = w_1 = M_{x1} = 0 \quad at \quad x = x_0, x_0 + L \\
&\lambda = \left(\frac{m\pi}{\ln(x_0 + L) - \ln x_0} \right) \\
&\phi = \lambda \ln\left(\frac{x}{x_0} \right) \\
&u_1 = A \sin^2\left(\lambda \ln\left(\frac{x}{x_0} \right) \right) = A \sin^2 \phi \qquad , x_0 \le x \le x_0 + L \\
&v_1 = B \sin\left(\lambda \ln\left(\frac{x}{x_0} \right) \right) \\
&w_1 = C\, x^{\left(\frac{1-v}{2}\right)} \sin\left(\lambda \ln\left(\frac{x}{x_0} \right) \right) = C\, x^k \sin\phi \qquad , k = \left(\frac{1-v}{2} \right)
\end{aligned}
\tag{26}
$$

where $m = 1, 2, 3, \ldots$ is the numbers of the meridional wave, and A and C are constant coefficients. The approximate solutions (26) are substituted in Eqs. (23), using the Galerkin minimization technique, to yield

$$
\begin{bmatrix} a_{11} & a_{13} \\ a_{31} & a_{33} \end{bmatrix} \begin{bmatrix} A \\ C \end{bmatrix} = \begin{bmatrix} 0 \\ 0 \end{bmatrix} \tag{27}
$$

where the coefficients a_{ij} are functions of geometric parameters of the conical shell. In order to obtain the critical axisymmetric buckling axial load one should set the determinant of the coefficient matrix to zero and solve the resulting equation. As seen from the definitions of constants a_{ij} , only a_{33} contains the axial load resultant that the coefficients a_{ij} are in Appendix.

$$
\begin{vmatrix} a_{11} & a_{13} \\ a_{31} & a_{33} \end{vmatrix} = 0 \tag{28}
$$

Therefor the critical axisymmetric buckling axial load is

$$
P_{cr} = \frac{\pi \sin 2\beta \left(a_{11} a'_{33} - a_{13} a_{31} \right)}{a_{11} \left[\left(2\lambda k - \lambda \right) \sin\beta Q_{18} + \left(k^2 - k - \lambda^2 \right) \sin\beta Q_{13} \right]} \tag{29}
$$

3 RESULTS AND DISCUSSION

Consider a porous truncated conical shell. The geometry is shown in Fig.1 the Young's Modulus and Poisson's ratio are, $E_0 = 70.6 Gpa, v = 0.3$, respectively. Simply supported boundary conditions are assumed. Show the dimensionless buckling axial compressive load versus the dimensionless parameter L / R_1. The classical buckling axial compressive load suggested by Seide and $E = E_0$ [2]

$$
F = \frac{2\pi E h^2 \cos^2 \beta}{\sqrt{3(1 - \nu^2)}} \tag{30}
$$

For the problem under consideration, the axisymmetric stability for mechanical buckling load of a porous conical shells presented. Fig.2 and Fig.3 show the variation of the buckling axial compressive load versus the dimensionless

parameter L / R_1 for different semi-vertex angles and coefficient porosity, respectively. The curves in Fig.2 show the critical axial loads increase as the semi-vertex angle decreases also the curves in Fig.3 show the critical axial loads increase when the coefficient of shell porosity decreases. From these figures they are found that by increasing values of L / R_1, the critical axial compressive load is decreased. Fig.4 indicated that increasing the thickness of the porous conical shell increase stability and buckling axial compressive load of porous conical shell.

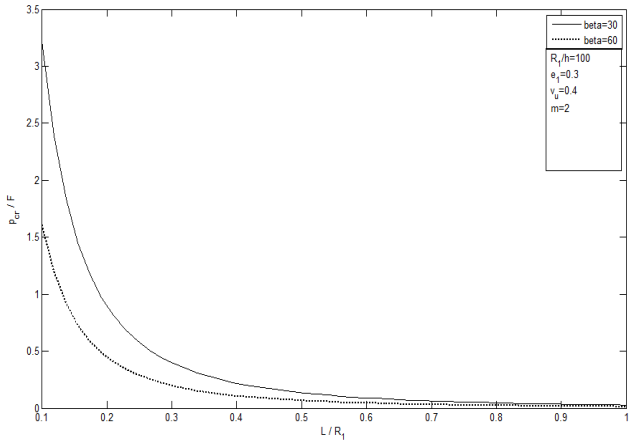

Fig.2
Variation of the dimensionless critical axial compressive load versus dimensionless parameter L / R_1 for stability of the porous conical shells in different semi-vertex angles (beta), $\beta = 30$ and $\beta = 60$.

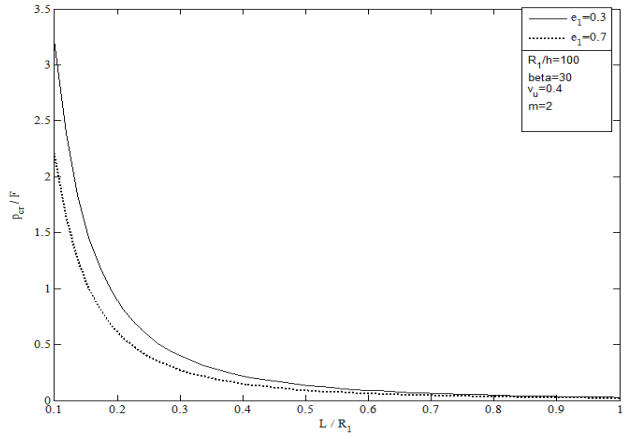

Fig.3
Variation of the dimensionless critical axial compressive load versus dimensionless parameter L / R_1 for stability of the porous conical shells in different coefficient porosity (e_1).

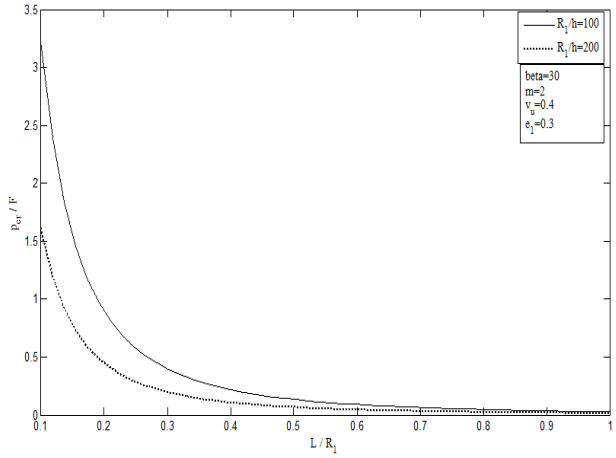

Fig.4
Variation of the dimensionless critical axial compressive load versus dimensionless parameter L / R_1 for stability of the porous conical shells in different dimensionless parameter radius versus thickness (R_1 / h).

Fig.5 shows variation of the dimensionless critical axial compressive load versus dimensionless parameter L / R_1 for stability of the porous conical shells that increasing numbers of the meridional wave decrease the stability and

critical axial compressive load. Fig.6 illustrated variation of the dimensionless critical axial compressive load versus dimensionless parameter L / R_1 for stability of the porous conical shells in different undrained Poisson's ratio (v_u), as decreasing undrained Poisson's ratio decreased the stability and critical axial compressive load.

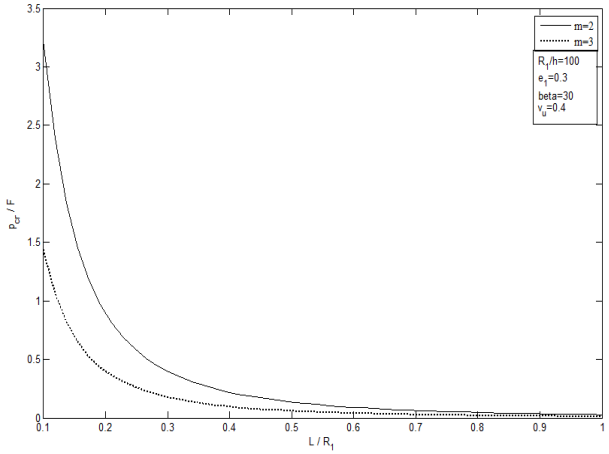

Fig.5
Variation of the dimensionless critical axial compressive load versus dimensionless parameter L / R_1 for stability of the porous conical shells in different numbers of the meridional wave (m).

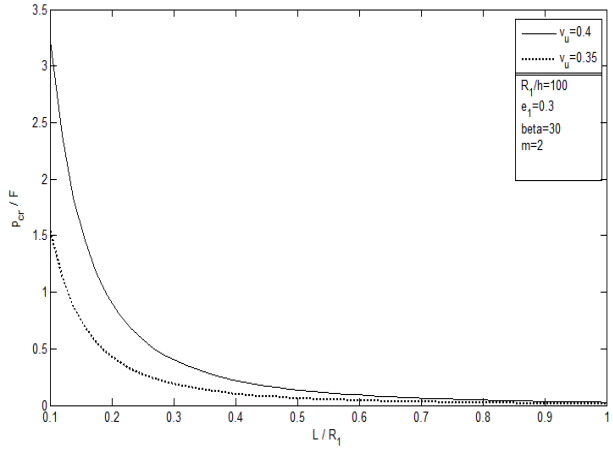

Fig.6
Variation of the dimensionless critical axial compressive load versus dimensionless parameter L / R_1 for stability of the porous conical shells in different undrained Poisson's ratio (v_u).

4 CONCLUSIONS

In the present article, the energy method is used for the mechanical buckling analysis of shell made of pore material and derivation is based on the first-order shell theory, Sanders kinematics equations and by using of variational formulations. The boundary condition of the shell are assumed to be clamped. The effects of coefficient porosity, semi-vertex angle, the meridional wave, undrained Poisson's ratio, thickness on critical load of truncated conical shell are presented and the conclusions are:

1. The critical axial load decreases and the shell will be unstable by increasing the porosity (e_1).
2. By increasing semi-vertex angles (β) critical axial load will be reduced.
3. The critical axial load increases by increasing the shell thickness (h).
4. The critical axial load decreases as the undrained Poisson's ratio decreased (v_u).
5. As the meridional wave (m) increase the critical axial load will be decreases.
6. By increasing dimensionless parameter L / R_1 The critical axial load decreases.

APPENDIX

$$A_2=\frac{1}{2}\int_{\frac{-h}{2}}^{\frac{h}{2}}\frac{A_1}{1-\alpha\beta}dz \quad , \quad A_3=\int_{\frac{-h}{2}}^{\frac{h}{2}}\frac{A_1}{1-\alpha\beta}\,z\,dz \quad , \quad A_4=\frac{1}{2}\int_{\frac{-h}{2}}^{\frac{h}{2}}\frac{A_1}{1-\alpha\beta}\,z^2dz$$

$$B_2=\int_{\frac{-h}{2}}^{\frac{h}{2}}\frac{B_1}{1-\alpha\beta}dz \quad , \quad B_3=\int_{\frac{-h}{2}}^{\frac{h}{2}}\frac{B_1}{1-\alpha\beta}z\,dz \quad , B_4=\int_{\frac{-h}{2}}^{\frac{h}{2}}\frac{B_1}{1-\alpha\beta}\,z^2dz$$

$$D_2=\int_{\frac{-h}{2}}^{\frac{h}{2}}G_{(Z)}\,dz \quad , \quad D_3=\int_{\frac{-h}{2}}^{\frac{h}{2}}G_{(Z)}\,z\,dz \quad , \quad D_4=\int_{\frac{-h}{2}}^{\frac{h}{2}}G_{(Z)}\,z^2dz$$

$$a_{11}=\sin\beta(B_2-2A_2)Q_1+\sin\beta(4\lambda^2A_2)Q_2$$

$$a_{13}=\sin\beta\left(\frac{(B_2-2A_2)(k+1)}{\tan\beta}-B_3k^2+B_3k+B_3\lambda^2\right)Q_3-\sin\beta\left(A_3k^3-4A_3k^2-B_3\lambda^2+4A_3k+4A_3\lambda^2-3A_3k\lambda^2+B_3k^2\right)Q_4$$

$$+\sin\beta\left(-2\lambda kB_3+\lambda B_3+\frac{\lambda B_2-2\lambda A_2}{\tan\beta}\right)Q_5+\sin\beta\left(-3A_3k^2\lambda+4A_3k\lambda+A_3\lambda^3-2A_3\lambda+B_32\lambda k-2B_3\lambda\right)Q_6$$

$$a_{31}=-\left(2A_2\cot\beta\right)\sin\beta Q_7+\sin\beta\left(B_3+A_3\right)Q_4-\sin\beta\left(\lambda B_3+\lambda A_3+\lambda B_2\cot\beta\right)Q_8-\sin\beta\left(4A_3\lambda^2\right)Q_9+\sin\beta\left(\lambda A_3-4A_3\lambda^3\right)Q_{10}$$

$$a_{33}=a'_{33}-\phi,$$

$$a'_{33}=\left(6kB_4+2kA_4\right)\sin\beta Q_{11}+\left(\frac{3B_3k}{\tan\beta}-4kA_4\right)\sin\beta Q_{12}+\begin{pmatrix}2B_3+\frac{A_3-B_3}{\tan\beta}-\frac{2A_2}{\tan^2\beta}+B_4k^2-B_4k\\-B_4\lambda^2+2A_4k^2-2A_4k-2A_4\lambda^2\end{pmatrix}\sin\beta Q_{13}$$

$$+\begin{pmatrix}2A_4k^4-12A_4k^3-2A_4\lambda^4+22A_4k^2-14A_4\lambda^2-6A_4k\lambda^2+12A_4k\lambda^2-8A_4k+6A_4\lambda^2\\-2k^3+6B_4k^2-4B_4k-6B_4\lambda^2-6A_4k^2+6B_4k\lambda^2+2A_4k^3\end{pmatrix}\sin\beta Q_{14}$$

$$+\left(6\lambda B_4+2\lambda A_4\right)\sin\beta Q_{15}+\left(\frac{3B_3\lambda}{\tan\beta}-4\lambda A_4\right)Q_{16}+\left(2B_4\lambda k-B_4\lambda+4A_4\lambda k-2A_4\lambda\right)\sin\beta Q_{17}$$

$$+\left(8A_4k^3\lambda-8A_4k\lambda^3-12A_4k^2\lambda-28A_4k\lambda-12A_4\lambda+8A_4\lambda^3\right)\sin\alpha Q_{18}$$

$$\phi=N_{xo}\left[\left(2\lambda k-\lambda\right)\sin\beta Q_{17}+\left(k^2-k-\lambda^2\right)\sin\beta Q_{13}\right]$$

$$Q_1=\int_{x_0}^{x_L}\sin^4\alpha\,dx \qquad Q_2=\int_{x_0}^{x_L}\cos2\alpha\sin^2\alpha\;\;dx \qquad Q_3=\int_{x_0}^{x_L}x^k\sin^3\alpha\,dx \qquad Q_4=\int_{x_0}^{x_L}x^{k-1}\sin^3\alpha\,dx$$

$$Q_5=\int_{x_0}^{x_L}x^k\cos\alpha\sin^2\alpha\,dx \qquad Q_6=\int_{x_0}^{x_L}x^{k-1}\cos\alpha\sin^2\alpha\;\;dx \qquad Q_7=\int_{x_0}^{x_L}x^k\sin^3\alpha\,dx \qquad Q_8=\int_{x_0}^{x_L}x^k\sin2\alpha\sin\alpha dx$$

$$Q_9=\int_{x_0}^{x_L}x^{k-1}\cos2\alpha\sin\alpha\,dx \quad Q_{10}=\int_{x_0}^{x_L}x^{k-1}\sin2\alpha\sin\alpha\,dx \qquad Q_{11}=\int_{x_0}^{x_L}x^{2k+2}\sin^2\alpha\,dx \qquad Q_{12}=\int_{x_0}^{x_L}x^{2k+1}\sin^2\alpha\,dx$$

$$Q_{13}=\int_{x_0}^{x_L}x^{2k-1}\sin^2\alpha\,dx \qquad Q_{14}=\int_{x_0}^{x_L}x^{2k-2}\sin^2\alpha\,dx \qquad Q_{15}=\int_{x_0}^{x_L}x^{2k+2}\sin\alpha\cos\alpha\,dx \quad Q_{16}=\int_{x_0}^{x_L}x^{2k+1}\sin\alpha\cos\alpha\,dx$$

$$Q_{17}=\int_{x_0}^{x_L}x^{2k-1}\sin\alpha\cos\alpha\,dx \quad Q_{18}=\int_{x_0}^{x_L}x^{2k-2}\sin\alpha\cos\alpha\,dx$$

REFERENCES

[1] Detournay E., Cheng A.H.D., 1993, *Fundamentals of Poroelasticity*, Chapter 5 in Comprehensive Rock Engineering: Principles, Practice and Projects, Vol. II, Analysis and Design Method, ed. C. Fairhurst, Pergamon Press.

[2] Seide P., 1956, Axisymmetric buckling of circular cones under axial compression, *Journal of Applied Mechanics* **23**: 625-628.

[3] Seide P., 1961, Buckling of circular cones under axial compression, *Journal of Applied Mechanics* **28**: 315-326.

[4] Singer J., 1961, Buckling of circular conical shells under axisymmetrical external pressure, *Journal of Mechanical Engineering Science* **3**: 330-339.

[5] Baruch M., Singer J., 1965, General instability of stiffened conical shells under hydrostatic pressure, *Aeronautical Quarterly* **26**: 187-204.

[6] Baruch M., Harari O., Singer J., 1967, Influence of in-plane boundary conditions on the stability of conical shells under hydrostatic pressure*, Israel Journal of Technology* **5**(1-2): 12-24.

[7] Baruch M., Harari O., Singer J., 1970, Low buckling loads of axially compressed conical shells, *Journal of Applied Mechanics* **37**: 384-392.

[8] Singer J., 1962, Buckling of orthotropic and stiffened conical shells, NASA TN D-1510: 463-479.

[9] Singer J., 1963, Donnell-type equations for bending and buckling of orthotropic conical shells, *Journal of Applied Mechanics* **30**: 303-305.

[10] Weigarten V.I., Seide P., 1965, Elastic stability of thin walled cylindrical and conical shells under combined external pressure and axial compression, *AIAA Journal* **3**: 913-920.

[11] Weigarten V.I., Seide P., 1965, Elastic stability of thin walled cylindrical and conical shells under combined internal pressure and axial compression, *AIAA Journal* **3**: 1118-1125.

[12] Ari-Gur J., Baruch M., Singer J., 1979, Buckling of cylindrical shells under combined axial preload, nonuniform heating and torque, *Experimental Mechanics* **19**: 406-410.

[13] Lu S.Y., Chang L.K., 1967, Thermal buckling of conical shells, *AIAA Journal* **5**(10): 1877-1882.

[14] Tani J., 1984, Buckling of truncated conical shells under combined pressure and heating, *Journal of Thermal Stresses* **7**: 307-316.

[15] Bhangale R., Ganesan N., Padmanabhan C.h., 2006, Linear thermoelastic buckling and free vibration behavior of functionally graded truncated conical shells, *Journal of Sound and Vibration* **292**: 341-371.

[16] Sofiyev A.H., 2007, Thermo-elastic stability of functionally graded truncated conical shells, *Composite Structures* **77**: 56-65.

[17] Naj R., Sabzikar M., Eslami M.R., 2008, Thermal and mechanical instability of functionally graded truncated conical shells, *Thin-Walled Structures* **46**: 65-78.

[18] Sofiyev A.H., Kuruoghlu N., Turkmen M., 2009, Buckling of FGM hybrid truncated conical shells subjected to hydrostatic pressure, *Thin-Walled Structures* **47**: 61-72.

[19] Sofiyev A.H.,2009, The vibration and stability behavior of freely supported FGM conical shells subjected to external pressure, *Composite Structures* **89**: 356-366.

[20] Sofiyev A.H., 2010, The buckling of FGM truncated conical shells subjected to combined axial tension and hydrostatic pressure, *Composite Structures* **92**: 488-498.

[21] Sofiyev A.H., 2010, Buckling analysis of FGM circular shells under combined loads and resting on the Pasternak type elastic foundation, *Mechanics Research Communications* **37**: 539-544.

[22] Sofiyev A.H., 2011, Thermal buckling of FGM shells resting on a two-parameter elastic foundation, *Thin-Walled Structures* **49**: 1304-1311.

[23] Bich D., Phoung N., Tung H., 2012, Buckling of functionally graded conical panels under mechanical loads, *Composite Structures* **94**: 1379-1384.

[24] Sofiyev A.H., 2011, Influence of the initial imperfection on the non-linear buckling response of FGM truncated conical shells, *International Journal of Mechanical Sciences* **53**: 753-762.

[25] Mirzavand B., Eslami M.R., 2011, A closed-form solution for thermal buckling of piezoelectric FGM hybrid cylindrical shells with temperature dependent properties, *Mechanics of Advanced Materials and Structures* **18**: 185-193.

[26] Jabbari M., Mojahedin A., Haghi M., 2014,Buckling analysis of thin circular FG plates made of saturated porous-soft ferromagnetic materials in transverse magnetic field, *Thin-Walled Structures* **85**: 50-56.

[27] Jabbari M., Farzaneh Joubaneh E., Mojahedin A.,2014,Thermal buckling analysis of porous circular plate with piezoelectric actuators based on first order shear deformation theory, *International Journal of Mechanical Sciences* **83**: 57-64.

[28] Jabbari M., Farzaneh Joubaneh E., Khorshidvand A.R., Eslami M.R., 2013, Buckling analysis of porous circular plate with piezoelectric actuator layers under uniform radial compression, *International Journal of Mechanical Sciences* **70**: 50-56.

[29] Magnucka-Blandzi E., 2008, Axi-symmetrical deflection and buckling of circular porous-cellular plate, *Thin-Walled Structures* **46**(3): 333-337.

[30] Liu P.S., 2011, Failure by buckling mode of the pore-strut for isotropic three-dimensional reticulated porous metal foams under different compressive loads, *Materials & Design* **32**(6): 3493-3498.

[31] Nguyen D.D., Pham H.C., Vu M.A., Vu D.Q., Phuong T., Ngo D.T., Nguyen H.T., 2015,Mechanical and thermal stability of eccentrically stiffened functionally graded conical shell panels resting on elastic foundations and in thermal environment, *Composite Structures* **132**: 597-609.

[32] Meyers C.A., Hyer M.W., 1991, Thermal buckling and postbuckling of symmetrically laminated composite plates, *Journal of Thermal Stresses* **14**: 519-540.